ORIGINAL RESEARCH

High-performance homogenized and spray coated nanofibrillated cellulose-montmorillonite barriers

Kirubanandan Shanmugam · Shaun Ang · Maisha Maliha ·
Vikram Raghuwanshi · Swambabu Varanasi · Gil Garnier · Warren Batchelor

Abstract Nanofibrillated cellulose (NFC) is a promising candidate for the development of high-performance renewable packaging. The water vapour permeability (WVP) of NFC sheets can be improved with the addition of inorganic nanoparticles such as montmorillonite nanoclay (MMT). However, these nanoparticles reduce the already poor sheet drainage when layers are formed through vacuum filtration. Spray-coating, on the other hand, is a recently developed rapid method for sheet formation. However, higher WVP of spray-coated NFC sheets compared to its vacuum filtered counterpart still remains a limitation. This work reports a new method for spray-coating a NFC-MMT composite sheet to improve both the ease of preparation and WVP barrier performance. Critically, the WVP of CNF sheets could be significantly reduced by processing the CNF-MMT suspension in a high-pressure homogenizer prior to spray-coating. X-ray diffraction measurements confirmed that the MMT particles were aligned in the plane of the sheet and were strongly interacting with the NFC matrix. At the optimal MMT loading of 20 wt%, WVP of 8.3×10^{-12} g/m s Pa was achieved. This resulted in comparable barrier performance to vacuum filtered NFC-MMT sheets, with the added benefit of being much easier to produce. Furthermore, spray-coating with 2 wt% suspension reduces the required water removal during drying by almost 90% (291 tonne water/tonne dry NFC product), compared to forming equivalent sheets using vacuum filtration at 0.3 wt%. The spray-coating process is of industrial interest as it is scalable and it is easy to engineer the properties of the NFC composites by varying the MMT content.

K. Shanmugam · S. Ang · M. Maliha ·
V. Raghuwanshi · S. Varanasi · G. Garnier ·
W. Batchelor (✉)
Department of Chemical Engineering, Bioresource
Processing Research Institute of Australia, Monash
University, Melbourne, VIC 3800, Australia
e-mail: warren.batchelor@monash.edu

Graphic abstract
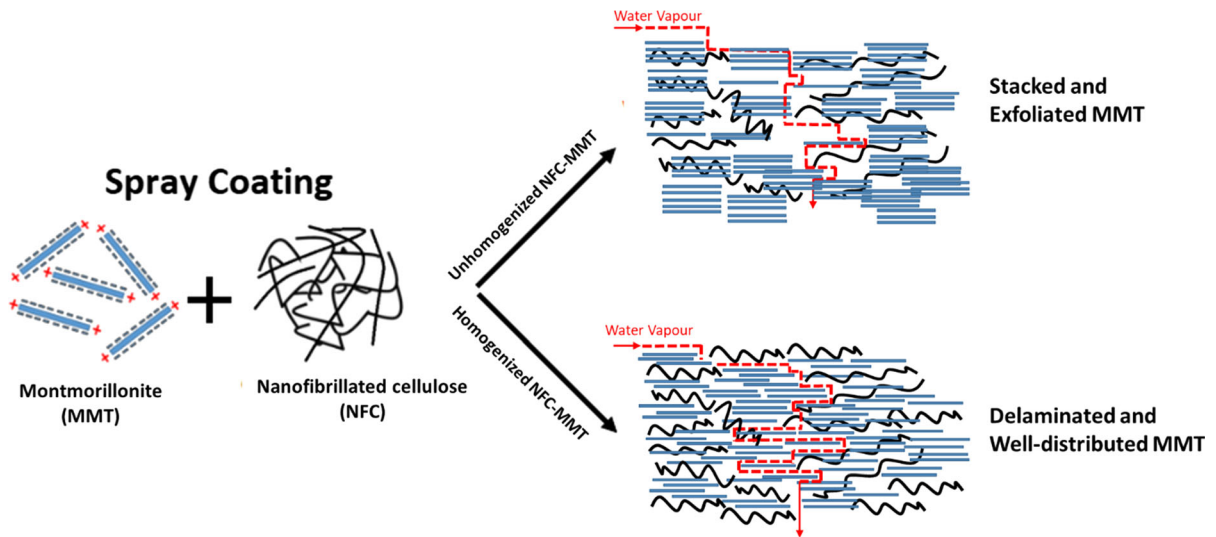
Introduction

Synthetic plastics are commonly utilised in conventional packaging materials for their good barrier properties against water vapour, oxygen, carbon dioxide, air and water (Silvestre et al. 2011). Despite this, plastics are often linked to a wide range of environmental issues such as poor biodegradability, poor recyclability and plastic microparticulate pollution. Undoubtedly, the need for more sustainable and renewable materials has never been more evident.

Cellulose is an abundant, renewable and eco-friendly biomaterial which has long been utilised in the paper, paperboards, container board, shipping sack and packaging industries (Berk 2013). While paper products have good mechanical properties, they often struggle with issues of poor barrier performance due to the large pores present in paper. These pores allow a significant amount of gas and water vapour to permeate through the fiber network, resulting in oxidation and poor shelf-life of foods and drugs. The barrier performance of paper products is often improved by use of wax coatings and synthetic plastic laminates such as low-density polyethylene and polypropylene. However, these coated and laminated paper composites are difficult to recycle and reprocess.

Recently, extensive research has been conducted in the field of nanofibrillated cellulose (NFC) as a high-performance barrier material due to its renewable and recyclable nature. NFC materials offer outstanding rigidity, tensile, flexural strength and barrier properties. NFC have high aspect ratio with the fibril diameter varying from 5 to 100 nm and length of a few microns. They form a highly compact network by entanglement via hydrogen bonding. The compact fibril network structure of NFC sheets offers a promising alternative to synthetic packaging materials as a barrier material (Henriksson et al. 2008).

While NFC sheets provide a good barrier against oxygen, they suffer from issues of high water vapour permeability (WVP) under medium and high humidity environments due to the hydrophilic nature of cellulose. The cellulose fiber–fiber bond in the fibril network swells through the absorption of water vapour. The swollen and weakened fibrous network expedites the diffusion pathway for water vapour. As a consequence, the WVP of a NFC sheet increases (Nair et al. 2014) and the stability of cellulose fibril network deteriorates (Spoljaric et al. 2014). To improve the WVP of NFC, inorganic fillers such as nanoclays have been researched and incorporated into the fibrous matrix. The presence of these layered nanoclays in the NFC matrix results in a high-performance nanocomposite which increases the tortuosity of the diffusive

path for a water vapour/gas molecule, resulting in high barrier performance (Azeredo 2009). These nanocomposites are stiff and strong with low gas permeability (Liu and Berglund 2012). The formation of a fiber matrix network with well-dispersed platelet aggregates is critical to obtain good barrier performance of the nanocomposite (Liu et al. 2011).

One of the most promising inorganic fillers is montmorillonite (MMT), an alumina-silicate layered clay hydrated bentonite (Jochen et al. 2006). MMT functions as a nanofiller by producing a structure in the composite that forces the transfer of air/oxygen/water molecules to follow a very tortuous path resulting in lower permeance (Uyama et al. 2003). High-performance NFC-MMT composites were previously prepared via vacuum filtration (Garusinghe et al. 2018). However, the time required to form these nanocomposites via vacuum filtration was long and unattractive as it varied from a minimum of 24 h to 4 days. These MMT nanoparticles were not easily retained during the dewatering stage of vacuum filtration, thereby resulting in sheets with unpredictable properties. Another limitation with filtration is the required separation of the sheet from the filter surface and subsequent manual handling before drying. As a conventional manufacturing method, a limited range of sheet basis weights of the composite can be fabricated using filtration, as the drainage time increases exponentially with sheet thickness and grammage (Shanmugam et al. 2017).

Recently, a rapid spray coating method was developed and successfully implemented to produce pure NFC sheets (Shanmugam et al. 2017, 2018) and NFC nanocomposite sheets with graphite carbon black for electrode applications (Benevent et al. 2014). Spray coating is a novel process to develop NFC nanocomposites and tailor their properties through the addition of specific nanoparticles or nanofillers. Further, the operation time for spray coating is independent of the NFC concentration and nanoparticle loading. One study reported that a $NFC-SiO_2$ sheet produced via spray coating could have its properties tailored by varying the SiO_2 loading between 0 and 33 wt% into the suspension (Krol et al. 2015). In that study however, vacuum filtration was applied after spray coating in order to fully dewater the sheet (Krol et al. 2015).

This work investigates the production of high-performance NFC nanocomposite barriers via spray coating. Here, a scalable, good WVP NFC nanocomposite barrier layer was shown to be achievable with much lower processing times compared to other available NFC sheet formation alternatives.

Experimental

Materials

NFC were obtained from DAICEL Chemical Industries Limited Japan as Celish KY-100S grade which has a 75 wt% moisture content and 25 wt% solids content. The NFC in Celish KY-100S were previously reported to have a mean fiber length of 8 µm, mean fiber diameter of approximately 70 nm and fiber aspect ratio of about 140 (Varanasi et al. 2013). MMT nanoclay was obtained from BYK Additives and Instruments, Germany via IMCD Australia Limited as Cloisite-Na + powder. The packed bulk density of Cloisite-Na + is 568 g/L with a dry particle size < 25 µm (d_{50}). X-ray results confirmed a d_{001} of 1.17 nm for the MMT nanoclay.

Preparation of NFC-MMT suspension

A 2 wt% NFC suspension was first made with 20 dry g of NFC and 980 g of distilled water. This 1000 g suspension was thoroughly mixed in a 3 L Mavis Engineering (Model No. 8522) standard disintegrator operating at 3000 rpm for 15,000 revolutions. All subsequent MMT addition was based on the NFC dry solids content and varied at a 5 wt%, 10 wt%, 20 wt% and 30 wt% loading. For example, a 10 wt% MMT loading would correspond to the further addition of 2 dry g of MMT powder into the 1000 g NFC suspension. The resulting NFC-MMT suspension was disintegrated again at 3000 rpm and 15,000 revolutions. For each MMT loading, two NFC-MMT batches were produced. One batch was directly sent for spray coating while the other was sent for high-pressure homogenization followed by spray coating.

For comparative purposes, two 2 wt% pure NFC suspensions (without MMT) were also made. The first suspension was directly sent for spray coating while the second suspension was sent for homogenization followed by spray coating. This was done to establish a baseline of pure NFC sheets which would allow for a

fair comparison to the NFC-MMT sheet barrier performance.

High-pressure homogenization

Homogenization of the NFC-MMT suspension was performed using a GEA Niro Soavi PANDAPLUS 2000 high-pressure homogenizer operating at 1000 bars for 2 passes. Homogenization was shown to be an effective tool to adequately delaminate the larger stacks of MMT within the NFC suspension while further aiding the fibrillation of the NFC itself. Homogenization of the pure NFC suspension was also performed at the same conditions.

Spray coating of NFC-MMT suspension and sheet production

Initially, the pure unhomogenized and homogenized 2 wt% NFC suspensions were spray coated on stainless-steel plates to form pure NFC sheets. This process was then repeated for the NFC-MMT suspensions to form the composite sheets.

In both cases, the suspension was spray coated on square stainless steel plates using a Wagner Pro 117 Professional Spray System at 200 bar with a moving conveyor operating at a fixed velocity of 1.25 ± 0.25 cm/s. A standard 517 spray nozzle was used resulting in an elliptical spray jet with a 50° angle and 22.5 cm suspension coverage. The distance from the nozzle to the surface of the square stainless-steel plate was fixed at 50 cm. During operation, the system was allowed to run to first achieve steady state and prevent any spray jet discontinuities. Multiple sheets could be successfully fabricated in under a minute. All wet spray coated sheets were left to air dry under ambient laboratory conditions. The dried sheets were then peeled from their respective stainless-steel plates resulting in a rough air-exposed surface and a corresponding smooth stainless-steel-exposed surface. The sheets were then conditioned at 50% RH and 23 °C for 24 h prior to property testing. The experimental setup for the spray coating system is shown in Fig. 1.

Sheet water vapour permeability

The ASTM E96/E96M-05 standard was used to evaluate the WVP of all sheets. All tests were performed at 50% RH and 23 °C. Prior to testing, all

sheets were oven dried for a minimum of 4 h at 105 °C. Thwing-Albert EZ Vapometer Permeability Cups were filled with 40 g of dried anhydrous $CaCl_2$. The NFC-MMT sheets were then cut into 70 mm diameter circles and were used to cover the cups. The weight of the entire cup, $CaCl_2$ and sheet was measured at 4 h intervals. The water vapour transmission rate (WVTR) was then measured based on the slope of the line between weight gain and time. The WVTR of sheets were then normalised with sheet thickness and converted into WVP. Each NFC-MMT sample was repeated for 3 replicates and the average WVP was calculated.

Sheet apparent density

The AS/NZS 1301.426 s:2015 standard test method was used to evaluate the apparent density of the spray coated composite sheets. The density of the composite was calculated as the ratio of basis weight (g/m^2) to mean thickness of the composite. A Lorentzen & Wettre AB Thickness Tester Type 21 was used to determine the thickness of the spray coated sheets. The mean thickness was calculated from 25 random points across the sheet surface. The composite sheet was then oven dried for 4 h at 105 °C in order to obtain the oven dried mass. The ratio of the oven dried composite sheet mass to sheet area provides the sheet basis weight (g/m^2).

Sheet structure via X-ray diffraction

X-Ray Diffraction (XRD) was conducted on MMT (Cloisite Na^+) powder, pure NFC sheets and spray coated homogenized NFC-MMT composite sheets using a D8 Advance with DAVINCI Design. The device operates at 40 kV and 40 mA with a Cu Kα X-Ray radiation source. A 0.02° step size and 2°/min scan speed were used to scatter the radiation from the instrument. The range of diffraction angles for investigation of MMT orientation in the composite varied from 2° to 34°. Bragg's law was used to evaluate the interlayer spacing of MMT. The equation for Bragg's law was given below,

$$d = n\lambda/2Sin\theta \tag{1}$$

where the d-spacing (nm) is the interlayer spacing, n is the order of diffraction, λ is the wavelength of the X-Ray beam (nm) and θ is the angle of incidence. The

Fig. 1 Experimental setup of spray coating system

area under the first peak in the XRD spectrum was evaluated with Origin Software Pro 9.1. The base line was first removed by the software. The corrected spectrum was then fitted with the Gaussian–Lorentzian fit to find the area under the first peak of the MMT region.

Sheet mechanical properties

An Instron Model 5965 Universal Testing Machine was used for stress–strain load measurements to determine the mechanical properties of the sheets. The composite sheets were cut into 100 mm long and 15 mm wide strips and tested in accordance with AS/NZS 1301.448 s:2007 standards at a fixed 10 mm/min elongation rate. The sheet tensile index (Nm/g) was calculated as the ratio of tensile strength (N/m) to basis weight (g/m^2). For each NFC-MMT sample, a minimum of 7 strips was tested to obtain a mean value with 95% confidence intervals.

Results and discussion

Sheet appearance

The spray coated NFC-MMT composite sheets produced were noted to be flexible, foldable and of uniform thickness. The physical appearance of the NFC-MMT sheet was increasingly yellow in colour, with increasing MMT content as shown in Fig. 2. The well-distributed deposition of MMT throughout the NFC matrix was also confirmed in the SEM images as

shown in Fig. 2. This is due to absorption spectra of MMT in the nanocomposites.

Fig. S1 in the supplementary information shows an SEM image of the air-exposed rough side and steel-exposed smooth side of the 30 wt% NFC-MMT homogenized composite and pure homogenized NFC sheet. From Fig. S1, the surface of the composite shows scattered MMT throughout the NFC network. After homogenizing both NFC and MMT, the NFC diameter decreased and the MMT was shown to be well dispersed within the NFC network. This results in a compact fibrous network with reduced porosity. Fig S2 in the supplementary information shows SEM images of the cross-sectional view of the NFC-MMT composites. These results are further supported by the XRD analysis of the composites which confirm the adequate dispersion of MMT throughout the NFC network.

Sheet water vapour permeability

Figure 3 shows the WVP of the spray coated NFC-MMT composite sheets. Here, the WVP values were also compared with the vacuum filtered NFC-MMT composite sheets previously reported in (Garusinghe et al. 2018). The error bars indicate 95% confidence intervals.

The initial average WVP of a spray coated unhomogenized pure NFC sheet was noted to be 2.5×10^{-11} g/m s Pa as shown in Fig. 3. This value is similar to the water vapor permeability of similar pure NFC sheets formed by spraying for packaging applications (Maliha et al. 2019). Here, the addition of 5 wt% MMT loading was shown to decrease this WVP
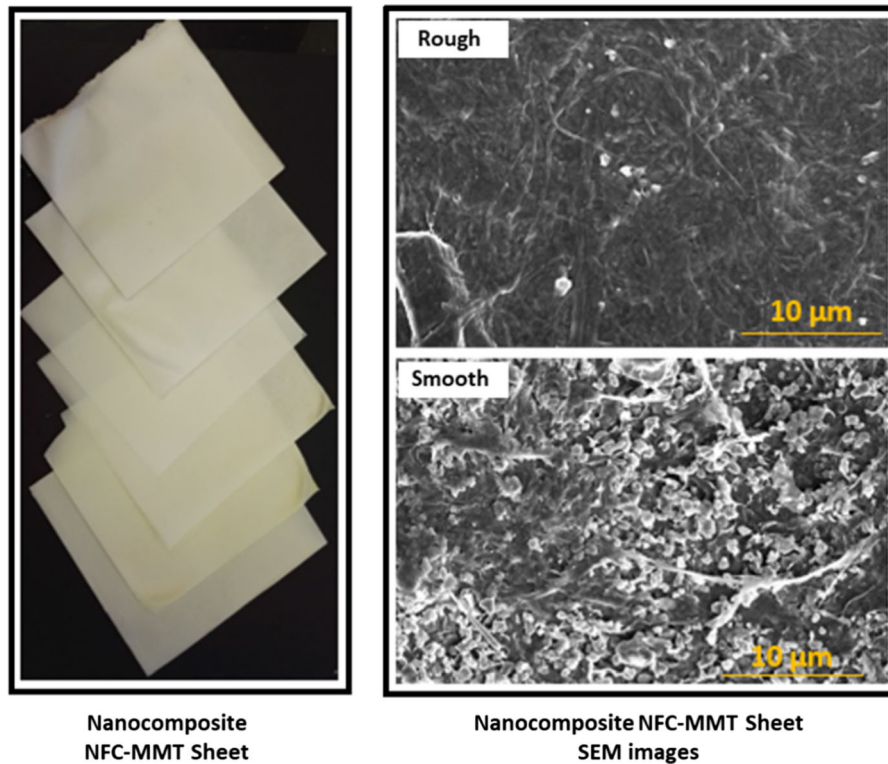
Fig. 2 Physical appearance and SEM images of spray coated NFC-MMT sheets

by more than half to 1.2×10^{-11} g/m s Pa. Beyond this loading however, the WVP increased to a maximum of 3.3×10^{-11} g/m s Pa at a 30% MMT loading. This is due to the presence of excessive MMT agglomeration as confirmed by the XRD results in the later sections of this paper.

Interestingly, homogenizing both the MMT and NFC suspension prior to spray coating yielded notable improvements to the WVP results at higher MMT loadings. At an optimum loading of 20% MMT, the average WVP of a spray coated homogenized NFC-MMT composite sheet was 0.8×10^{-11} g/m s Pa, as shown in Fig. 3. It is believed that the process of homogenization breaks down and delaminates the larger MMT particles, thereby increasing their effective surface area (Garusinghe et al. 2018). This in return results in a more even distribution of MMT throughout the NFC matrix which increases the overall tortuosity of the pathway for the permeance of water vapour (Garusinghe et al. 2018). Here, the performance of the spray coated NFC-MMT sheet at 0.8×10^{-11} g/m s Pa was very close to that of the

best vacuum filtered NFC-MMT sheet at about 0.6×10^{-11} g/m s Pa.

Sheet apparent density

Figure 4 shows the sheet apparent density values obtained for the spray coated NFC-MMT composite sheets alongside the vacuum filtered sheets (Garusinghe et al. 2018). The error bars indicate 95% confidence intervals.

As shown in Fig. 4, the apparent density of all composite sheets prepared by spray coating were lower than their corresponding vacuum filtered counterparts. The nanofibers in the pure spray coated sheets tend to form small agglomerates and clumps with the spray coating process as previously reported (Shanmugam et al. 2018) which reduces sheet packing density.

This issue is further exacerbated at high MMT loading quantities as shown in Fig. 4. Here, approximately similar sheet apparent density values were obtained despite the increased MMT load for the unhomogenized spray coated NFC-MMT composite
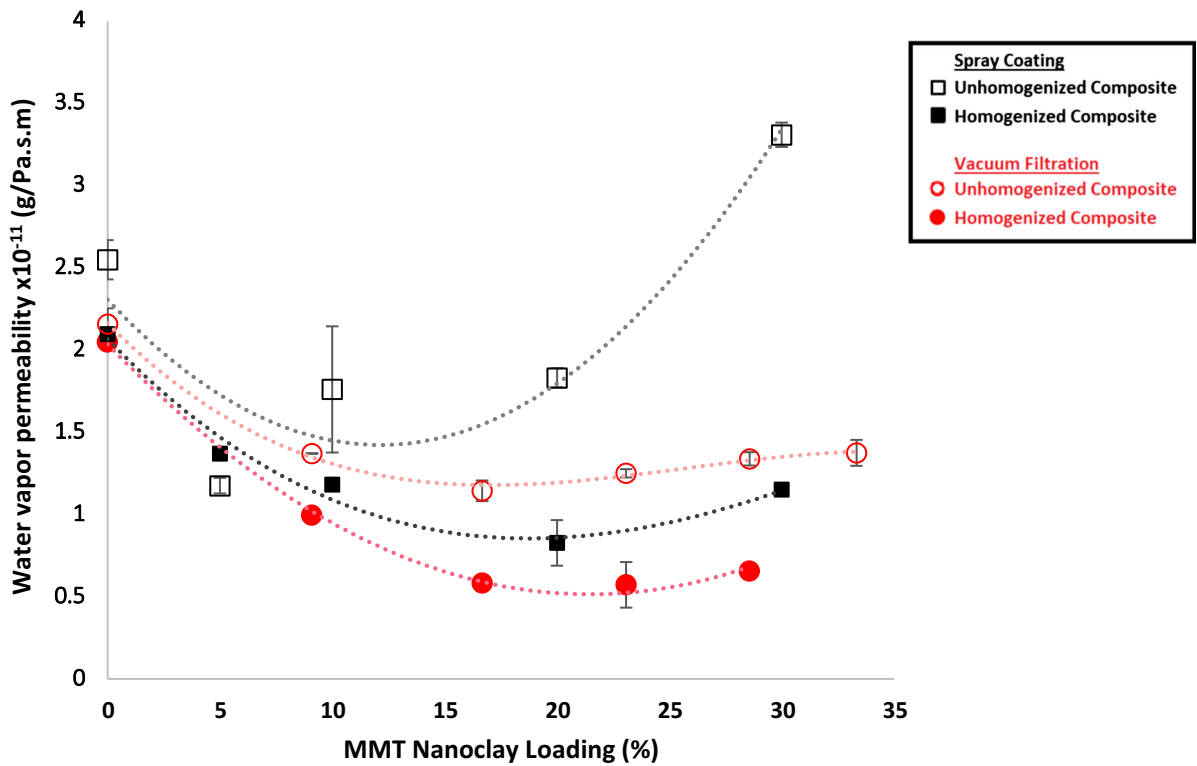
Fig. 3 Water vapour permeability of spray coated and vacuum filtered NFC-MMT sheets containing the same amount of NFC with varying additional MMT loading with respect to the NFC content
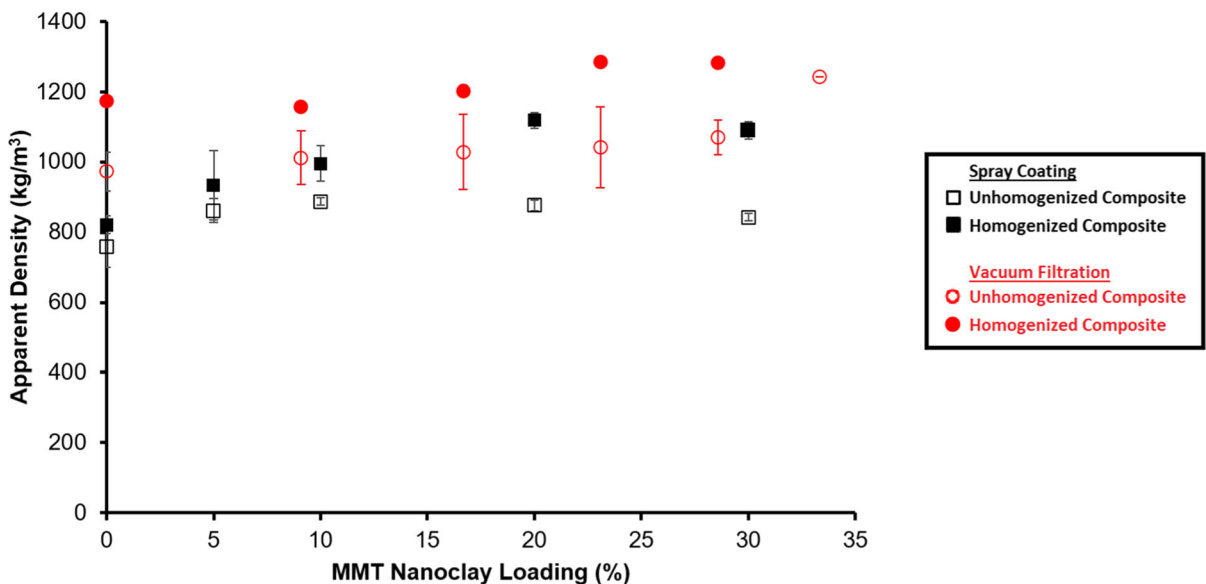

Fig. 4 Apparent density of spray coated and vacuum filtered NFC-MMT sheets

sheet. As previously mentioned, it is believed that the MMT has an increased affinity to form larger stacks at very high loading (Garusinghe et al. 2018). This disrupts the overall packing structure which results in

the increased WVP as shown in Fig. 3. At optimally lower MMT loads however, the nanoclay is able to fill gaps within the fiber network which improves the overall packing structure.

Evidently, the process of homogenization resulted in improved sheet apparent density for all spray coated and vacuum filtered cases. The high mechanical shearing forces in a homogenizer were noted to be effective in breaking down the larger MMT stacks and adequately dispersing them throughout the NFC-MMT suspension. This in return results in a more tightly packed sheet structure which increases the sheet apparent density.

Sheet structure

XRD analysis was performed on the spray coated NFC-MMT composites in order to determine the orientation of MMT in the NFC network. Figure 5 shows the XRD patterns of pure MMT, pure NFC and NFC-MMT composites under all MMT loadings. The area under the curve (AUC) provides information on the amount of MMT present in the composite and increases with MMT loading. The AUC of the first peak was chosen because MMT produces a peak from 2° to 10°, which represents the spacing between the MMT layers. As shown in Fig. 5, pure NFC had no characteristic peak in the range of 2° to 10°.

From Fig. 5, the AUC increases sharply from the pure MMT to 10 wt% MMT loading. This is due to the alignment of MMT in the plane of the sheets. In its pure powdered state, MMT is aligned randomly and only flat-oriented platelets will contribute to the diffraction pattern. A more thorough comparison of the AUC of the first peaks in the XRD spectrum versus the MMT loading for the unhomogenized and homogenized composites can be found in Fig. S3 and Fig. S4, respectively in the supplementary information.

Figure 6 shows the effect of MMT loading on the d-spacing of MMT in the composites. The d-spacing of pure MMT was evaluated to be 11.78 Å from the diffraction peak at $2\theta = 7.5°°$ using Eq. 1. The orientation of MMT platelets in the composite shows a peak in this range. The interspacing of MMT platelets barely varies from 14.7 to 14.2 Å in the homogenized composites as the MMT content was increased from 10 wt% to 30 wt%. This reveals a strong interaction of MMT platelets and the NFC fiber network. The interspacing is constant and independent of MMT loading, except for the 5 wt% homogenized composite. The effect of charge distribution between the MMT and nanocellulose can be one possible reason for the variation in the MMT interlayer spacing. The diffraction peak of MMT in the 5 wt% and 10 wt% unhomogenized composites were 6.06° and 6.20°, respectively. There is no peak for the 5 wt%
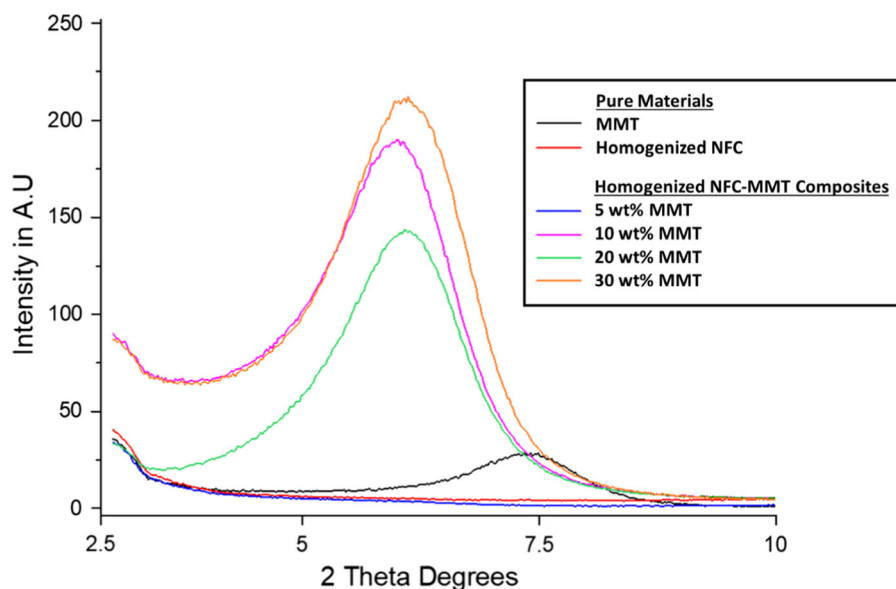

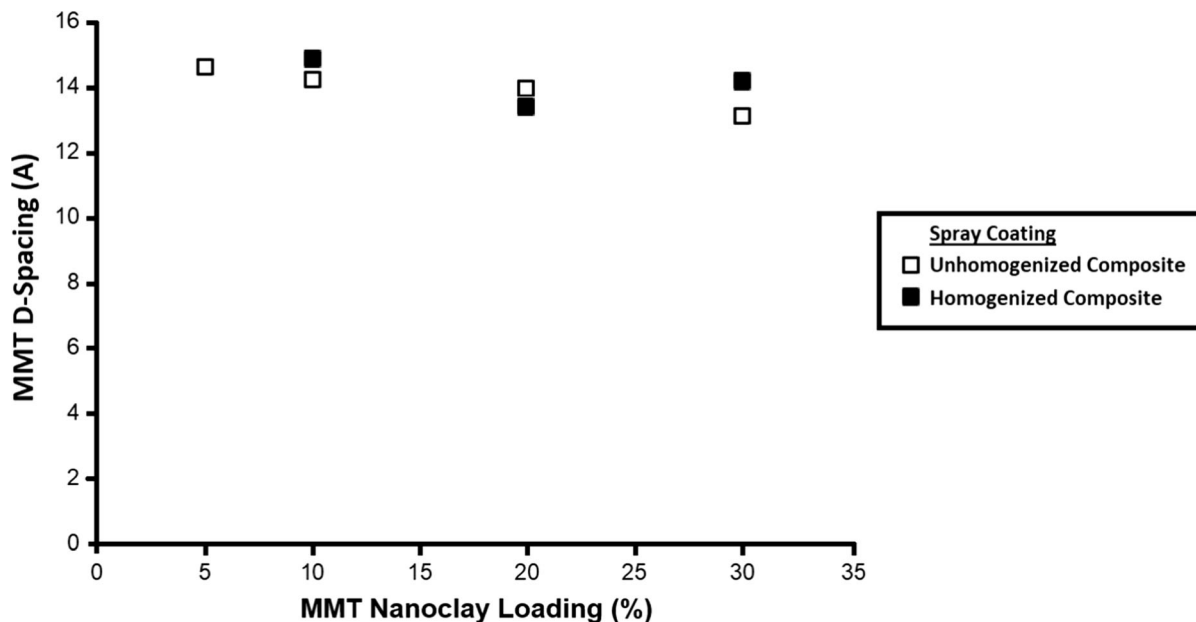**Fig. 5** First peak in the XRD spectrum of pure MMT, pure NFC and NFC-MMT composites

Fig. 6 Effect of MMT loading on the d-spacing of MMT at the first peak in the XRD spectrum

homogenized sample and a peak at 6.06° for the 10 wt% homogenized composites. The absence of the peak in 5 wt% homogenized composite suggests that MMT platelets completely lose their arrangement on homogenization and are fully dispersed in the CNF fibrous matrix. The composite beyond 5 wt% had peak values due to the stacking of MMT platelets and their subsequent alignment in the plane of the NFC sheet. Thereafter, peak positions increased slightly with MMT content for both types of composites. This means that all the MMT will contribute to the scattering, whereas with pure MMT only the small fraction of platelets that orient in the plane will contribute.

Sheet mechanical properties

Figure 7 shows the tensile index of the NFC-MMT composite sheets as a function of MMT nanoclay loading for both unhomogenized and homogenized cases. The error bars indicate 95% confidence intervals. It is worth noting that the aim of this mechanical strength study was to demonstrate that the addition of an optimum amount of MMT nanoclay does not adversely affect sheet strength.

In the case of the unhomogenized composite, the addition of up to 10 wt% MMT resulted in slight improvements to the sheet tensile index (55 Nm/g) compared to that of the pure NFC sheet (48 Nm/g). However, a decrease in sheet strength performance was observed past a loading of 20 wt% MMT, consistent with the decrease in WVP barrier performance values in the previous section.

In the case of the homogenized composite, the addition of up to 20 wt% MMT resulted in relatively similar sheet tensile index values compared to that of the pure NFC sheet at about 80 Nm/g. The increased tensile index values of homogenized sheets over unhomogenized sheets is due to the increased degree of NFC fibrillation which increases the number of fiber–fiber bonds and the overall capacity of the fiber sheet network to bear load (Ang et al. 2019). A decrease in sheet strength performance was also observed past the optimal 20 wt% MMT loading point and is also consistent with the decrease in WVP barrier performance values in previous section.

Here, we have demonstrated that at the optimal level of MMT loading, the high strength properties of the composite sheet can be retained while still resulting in good sheet barrier performance. The tensile strength and E-modulus of spray coated composites can be found in Fig. S5 and Fig. S6 in the supplementary information.
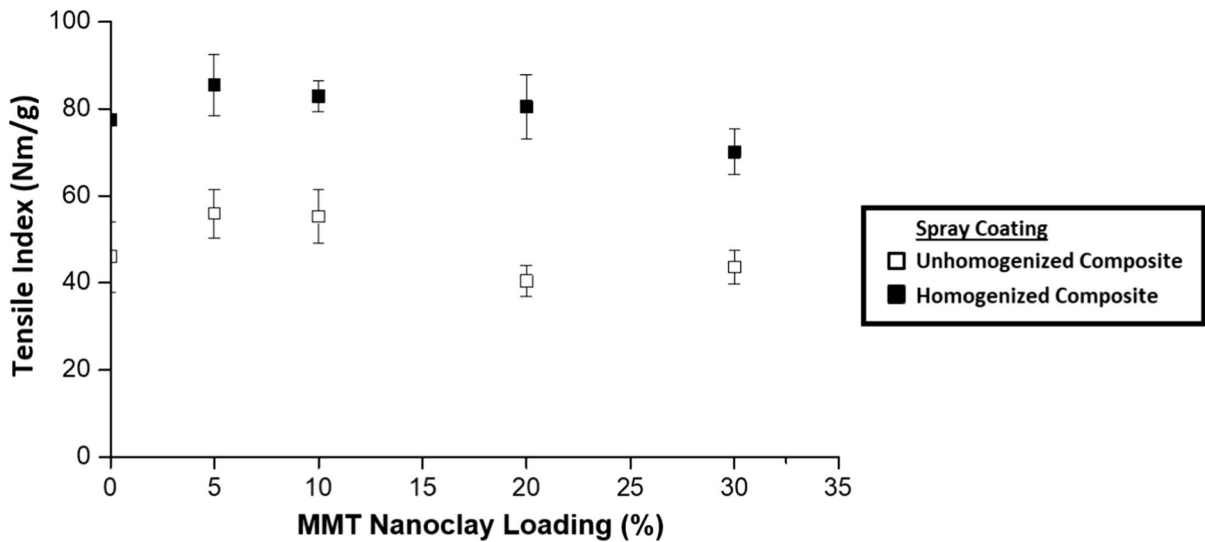
Fig. 7 Tensile index of NFC-MMT composite sheets as a function of MMT nanoclay loading

Novelty of process

To the best of our knowledge, there are no readily available industrial methods for the rapid production of NFC composite sheets. The most common method for the fabrication of NFC composites is by use of vacuum filtration. Vacuum filtration is often performed in laboratory-scale settings and has numerous drawbacks. As noted in a previous study, the addition of MMT nanoclays into a 0.3 wt% NFC suspension drastically increased the sheet dewatering time with vacuum filtration from 30 min to 24 h (Garusinghe et al. 2018). Further, the manual-peeling process employed to separate a drained nanocomposite sheet from its filter often leads to surface defects. These issues hinder the rapid production of NFC composite sheets such as NFC-MMT on a commercial scale.

Among the various sheet fabrication technologies, spray coating presents as a viable solution to rapidly form NFC composite sheets. It has the added benefit of being flexible in handling high NFC suspension consistencies compared to vacuum filtration (Shanmugam et al. 2017). As demonstrated in our previous work with pure NFC, the operation time for spray coating was less than 1 min (Shanmugam et al. 2018). This spray coating process could be scalable for the production of self-standing composites or for laminating composites onto a base sheet (Mirmehdi et al. 2018). The spraying of NC onto a continuous steel substrate followed by rapid drying on the same

substrates would be a feasible process. The sheets can be dried in 5 h at 50 °C as reported in our previous work and can be reduced to up to 2 h for modified composites at higher temperatures (Nadeem et al. 2020). In industrial practice, the waste heat recovered to dry the wet film from spraying through the tunnel dryer. Additionally, Yankee dryer and Condebelt technology can be applied for continuous drying process of wet film (Stenström 2019).

Spray coating also drastically reduces the water consumption and water removal required with conventional filtration. For example, vacuum filtering a 0.3 wt% NFC suspension (0.3 g dry fiber in 99.7 g water) requires the removal of 332 tonne water/tonne fiber. In our study, a 2 wt% NFC suspension coupled with an optimum 20 wt% MMT loading (based on dry NFC weight) equates to a total solids content of 2.4 wt% (2.4 g dry fiber in 97.6 g water), which requires the removal of 41 tonne water/tonne fiber. Ultimately, this equates to an almost 90% reduction (291 tonne water/tonne fiber) in water removal requirements using spray coating as opposed to conventional vacuum filtration. However, the water removal mechanism is different in both cases. In the case of vacuum filtration, the water removal can be achieved at the wet end of a paper machine. On the other hand, for spraying evaporative removing of water is required. While this is a promising approach for preparation of high-performance barrier material in terms of material performance and ease of

preparation, future studies to evaluate the energy requirements and the economic feasibility of the process are required.

Conclusion

In this study, homogenized NFC-MMT composite sheets were spray coated onto impermeable stainless-steel surfaces and their barrier and strength properties were investigated. The resulting NFC-MMT composite sheets had good WVP barrier performance of 8.3×10^{-12} g/m s Pa at an optimal 20 wt% MMT loading. This WVP value was comparable to that obtained from vacuum filtered NFC-MMT composite sheets. Further, spray coating reduced the required water removal during drying by almost 90% (291 tonne water/tonne dry NFC product), compared to forming equivalent sheets using vacuum filtration at 0.3 wt%. XRD analysis confirmed that homogenization was effective in breaking down the larger stacks of MMT nanoclays leading to an even-distribution of MMT throughout the NFC fiber matrix. Even at a high 20 wt% MMT loading, the high mechanical strength of the spray coated NFC-MMT sheets was similar to that of pure NFC sheets at about 80 Nm/g.

Here, we have successfully demonstrated that a high-performance NFC-MMT barrier material can be feasibly and rapidly made by spray coating. Further, the MMT loading quantities have no effect on the operation time for spray coating. This creates a range of opportunities to flexibly tailor the properties of nanocomposite sheets for packaging applications.

Supplementary material

This manuscript contains the following supplementary materials: The 1 µm micrographs of spray coated composites (Fig. S1), cross-sectional micrograph of spray coated composites (Fig. S2), XRD spectrum of unhomogenized composites (Fig. S3), plot between area under the curve (AUC) of first peak vs MMT loading (Fig. S4) and mechanical properties of spray coated composites (Fig. S5 and Fig. S6).

References

Ang S, Haritos V, Batchelor W (2019) Effect of refining and homogenization on nanocellulose fiber development, sheet strength and energy consumption. Cellulose 26:4767–4786. https://doi.org/10.1007/s10570-019-02400-5

Azeredo HMCD (2009) Nanocomposites for food packaging applications. Food Res Int 42:1240–1253. https://doi.org/10.1016/j.foodres.2009.03.019

Beneventi D et al (2014) Pilot-scale elaboration of graphite/microfibrillated cellulose anodes for Li-ion batteries by spray deposition on a forming paper sheet. Chem Eng J 243:372–379. https://doi.org/10.1016/j.cej.2013.12.034

Berk Z (2013) Chapter 27—Food packaging. In: Berk Z (ed) Food process engineering and technology, 2nd edn. Academic Press, San Diego, pp 621–636. https://doi.org/10.1016/B978-0-12-415923-5.00027-7

Garusinghe UM, Varanasi S, Raghuwanshi VS, Garnier G, Batchelor W (2018) Nanocellulose-montmorillonite composites of low water vapour permeability. Colloids Surf A Physicochem Eng Asp 540:233–241. https://doi.org/10.1016/j.colsurfa.2018.01.010

Henriksson M, Berglund LA, Isaksson P, Lindström T, Nishino T (2008) Cellulose nanopaper structures of high toughness. Biomacromol 9:1579–1585. https://doi.org/10.1021/bm800038n

Jochen W, Paul T, Julian MD (2006) Functional materials in food nanotechnology. J Food Sci 71:R107–R116. https://doi.org/10.1111/j.1750-3841.2006.00195.x

Krol LF, Beneventi D, Alloin F, Chaussy D (2015) Microfibrillated cellulose-SiO2 composite nanopapers produced by spray deposition. J Mater Sci 50:4095–4103. https://doi.org/10.1007/s10853-015-8965-5

Liu A, Berglund LA (2012) Clay nanopaper composites of nacre-like structure based on montmorrilonite and cellulose nanofibers—improvements due to chitosan addition. Carbohydr Polym 87:53–60. https://doi.org/10.1016/j.carbpol.2011.07.019

Liu A, Walther A, Ikkala O, Belova L, Berglund LA (2011) Clay nanopaper with tough cellulose nanofiber matrix for fire retardancy and gas barrier functions. Biomacromol 12:633–641. https://doi.org/10.1021/bm101296z

Maliha M et al (2019) Bismuth phosphinate incorporated nanocellulose sheets with antimicrobial and barrier properties for packaging applications. J Clean Prod. https://doi.org/10.1016/j.jclepro.2019.119016

Mirmehdi S, Hein PRG, de Luca Sarantópoulos CIG, Dias MV, Tonoli GHD (2018) Cellulose nanofibrils/nanoclay hybrid composite as a paper coating: effects of spray time, nanoclay content and corona discharge on barrier and

mechanical properties of the coated papers. Food Packag Shelf Life 15:87–94

Nadeem H et al (2020) An energy efficient production of high moisture barrier nanocellulose/carboxymethyl cellulose films via spray-deposition technique. Carbohydr Polym 250:116911. https://doi.org/10.1016/j.carbpol.2020.116911

Nair SS, Zhu J, Deng Y, Ragauskas AJ (2014) High performance green barriers based on nanocellulose. Sustain Chem Process 2:23. https://doi.org/10.1186/s40508-014-0023-0

Shanmugam K, Varanasi S, Garnier G, Batchelor W (2017) Rapid preparation of smooth nanocellulose films using spray coating. Cellulose 24:2669–2676. https://doi.org/10.1007/s10570-017-1328-4

Shanmugam K, Doosthosseini H, Varanasi S, Garnier G, Batchelor W (2018) Flexible spray coating process for smooth nanocellulose film production. Cellulose 25:1725–1741. https://doi.org/10.1007/s10570-018-1677-7

Silvestre C, Duraccio D, Cimmino S (2011) Food packaging based on polymer nanomaterials. Prog Polym Sci 36:1766–1782

Spoljaric S, Salminen A, Dang Luong N, Lahtinen P, Vartiainen J, Tammelin T, Seppälä J (2014) Nanofibrillated cellulose, poly(vinyl alcohol), montmorillonite clay hybrid nanocomposites with superior barrier and thermomechanical properties. Polym Compos 35:1117–1131. https://doi.org/10.1002/pc.22759

Stenström S (2019) Drying of paper: a review 2000–2018. Drying Technol. https://doi.org/10.1080/07373937.2019.1596949

Uyama H, Kuwabara M, Tsujimoto T, Nakano M, Usuki A, Kobayashi S (2003) Green nanocomposites from renewable resources: plant oil–clay hybrid materials. Chem Mater 15:2492–2494. https://doi.org/10.1021/cm0340227

Varanasi S, He R, Batchelor W (2013) Estimation of cellulose nanofibre aspect ratio from measurements of fibre suspension gel point. Cellulose 20:1885–1896. https://doi.org/10.1007/s10570-013-9972-9